THE ASTROPHYSICAL JOURNAL, 264:373–391, 1983 January 15

SUPERCLUSTERS AS NONDISSIPATIVE PANCAKES: FLATTENING

AVISHAI DEKEL
Theoretical Astrophysics, California Institute of Technology
Received 1982 March 5; accepted 1982 July 9

ABSTRACT

The formation and dynamical evolution of flat superclusters (SCs) out of adiabatic perturbations of the Zel'dovich type are studied by means of N-body simulations in an Einstein–de Sitter universe, and by an approximate model in an open universe. A nondissipative formation scenario, in which galaxies or other substructures form prior to the collapse of SCs from small-scale perturbations, is found to be compatible with the observed flattening of the Local Supercluster (LSC) and of external SCs, and with their pancake-halo structure. In the best fitting model the LSC has collapsed in one dimension only recently, where 20–50% of the galaxies have crossed the plane by now, corresponding to a caustic at $0 < z < 0.5$. The flattening is found to be nontransient even with no dissipation, and is expected to become even more pronounced for quite a few collapse times until rich clusters determine the thickness of the pancake or until possible turnaround in the SC plane. The dissipative pancake scenario, in which galaxies form due to the SC collapse (possibly inside a halo of massive neutrinos), leads to a too flat distribution of galaxies, but this may be an artifact of the idealized initial conditions assumed here.

An approximate model which is based on the formalism of Zel'dovich before the first collapse, and makes use of adiabatic invariants at later stages, agrees well with the numerical simulations, and provides a useful tool for the study of the postcollapse evolution of SCs.

Subject headings: cosmology — galaxies: clusters of — galaxies: formation

I. INTRODUCTION

Observations indicate that galaxies and clusters are embedded in 10^{15}–10^{16} $M_\odot$ superclusters (SCs), which commonly consist of *flat* central components that extend to a few tens of Mpc along their long axes, but are only a few Mpc thick (see an extensive review by Oort 1982). The progenitors of SCs are believed to be primordial, *adiabatic* density perturbations in which radiation and matter are perturbed alike. Adiabatic perturbations on scales smaller than a critical mass, $M_D \sim 10^{15}$ $M_\odot$, have been damped out either by photon diffusion and viscosity prior to the plasma recombination if the universe is dominated by baryons (cf. Silk 1968; Peebles and Yu 1970), or alternatively by collisionless damping of relativistic neutrinos if they have a mass of ~ 30 eV and they dominate the universe (cf. Bond, Efstathiou, and Silk 1980; Doroshkevich *et al.* 1981). The smallest among the adiabatic perturbations that have survived the damping, which presumably had the highest amplitudes, were the first to grow and eventually form large-scale SCs. The collapse of such a proto-SC was likely to proceed in one dimension first, because of initial anisotropies (Zel'dovich 1970; Doroshkevich 1970) and their strong amplification during the collapse (Lynden-Bell 1962; Lin, Mestel, and Shu 1965; Oort 1970; Icke 1973), leading to a thin, highly dense sheet of material (caustic) at some finite time, t_c, which may still be expanding in the orthogonal directions.

The study of the formation and dynamical evolution of SCs is guided here by the question of the *origin of galaxies* and other substructures: were they formed as a result of the collapse of SCs, or independently, prior to that collapse? The former is advocated by Zel'dovich and his colleagues (cf. Sunyaev and Zel'dovich 1972; Doroshkevich, Shandarin, and Saar 1978) who suggest the formation of *pancakes* that stay thin due to gas dissipation. The pancakes, accreting more gas and being compressed and heated by shocks, eventually fragmented, and galaxies were formed in a very thin layer with very low normal velocities. A fashionable version of this scenario assumes that these dissipative pancakes form in the potential wells of dissipationless halos made of ~ 30 eV neutrinos (cf. Doroshkevich *et al.* 1981). The alternative picture suggests that galaxies were formed independently, i.e., from *isothermal* perturbations in the baryon density on smaller scales (cf. Peebles and Dicke 1968; Peebles 1974; White and Rees 1978), or, as may be suggestive in recent theories of the early universe, from adiabatic perturbations that may arise on galactic scales if the universe is dominated by exotic ~ 1 keV collisionless particles such as gravitinos, photinos, or right-handed neutrinos (Bond, Szalay, and Turner 1982; Blumenthal, Pagels, and Primack 1982). If a collapsing

SC was already made of such discrete bodies that interact mostly via gravitation, there was much less dissipation associated with the collapse, and the resultant galaxy distribution is expected to be somewhat thicker, with higher normal velocities. Note further than if galaxy formation was triggered by the SC collapse, it should have happened before $z \sim 3$ as required by lower limits on the ages of galaxies (e.g., from the range of quasar redshifts, and from evolutionary models of galaxies and star clusters), while there is no such requirement on the dynamical age of SCs in the nondissipative scenario. Hence, the observed properties of SCs may help us to distinguish between the theoretical scenarios for galaxy formation.

The approximate formalism of Zel'dovich (or alternatively the homogeneous ellipsoid approximation; see White and Silk 1979) allows one to follow the evolution semianalytically with a reasonable accuracy through the linear growth and up to t_c, but it breaks down after t_c when mixing occurs (cf. Doroshkevich *et al.* 1980). In order to study the postcollapse evolution, we have performed a series of numerical experiments based on a three-dimensional N-body code, which we then compare with a simple analytical model. This model is used to generalize the results. The experiment simulates a dissipationless scenario, but it can as well (but with some caution) be interpreted as simulating the dissipative scenario by identifying a proper dissipative pancake component at t_c (when galaxies are assumed to form dissipatively), and following its subsequent dissipationless evolution inside a massive halo (of neutrinos?).

In the present paper we focus on the global shape of SCs, which is their most reliably observed property. It becomes clear at a first glance that the disk-halo structure of SCs (e.g., 60% of the galaxies are in a flat component and 40% are in an extended, spherical halo in the Local Supercluster [LSC], according to Tully 1982) poses a difficulty to the pure dissipative pancake scenario; i.e., where do the halo galaxies come from? A scenario in which galaxies precede SCs provides a natural explanation, but the dissipative scenario can still be modified to allow galaxy formation in smaller pancakes during the large-scale collapse, and hence remove that difficulty.

The two scenarios are confronted here with the observed *flattening* of the LSC (cf. de Vaucouleurs 1978) which has been measured by Yahil, Sandage, and Tammann (1980) and by Tully (1982), and with preliminary estimates of apparent flattening in external SCs. It is found that a nondissipative scenario, which starts off with probable initial conditions, provides a pancake flat enough that it is not transient but rather stays very flat as long as expansion goes on in the pancake plane. In the best fitting model the LSC is young: it has collapsed to a caustic between $z = 0.5$ and now, and will become flatter in the future. The dissipative pancake scenario would have led to too flat systems if the initial conditions assumed here are not too far from reality.

In § II the formalism of Zel'dovich is summarized, and a simple estimate for the postcollapse evolution is suggested. The experiment is described in § III, and the evolution of flattening is studied in comparison with observations in § IV. The analytical model is checked in § V and is applied to an open universe. The results are discussed in § VI and summarized in § VII. Further aspects of the evolution of SCs, such as the velocity fields, the clustering and correlation functions, and the influence of the flattening on peculiar motions, overdensity, and forces in regard to derivations of Ω_0, are studied in associated papers (see § VII).

II. EVOLUTION OF ADIABATIC PERTURBATIONS

a) Zel'dovich's Formalism

We first summarize the formalism developed by Zel'dovich (cf. 1970, 1978) to treat the growth of nonspherical, adiabatic perturbations in a Friedmann universe. The formalism converges to the conventional linear theory in the linear regime, but remains a good approximation in the nonlinear phase as well until the collapse to a plane.

The position of every particle in space (i.e., Eulerian coordinates), $\boldsymbol{r}$, is given as a function of its comoving position (i.e., initial or Lagrangian coordinates), $\boldsymbol{q}$, and of time, t, by

$$\boldsymbol{r} = a(t)[\boldsymbol{q} - b(t)\psi(\boldsymbol{q})]. \tag{1}$$

The first term corresponds to a Hubble expansion, while the second term describes the displacement of the particle from its unperturbed position. The split to a spatial-dependent part, $\psi(\boldsymbol{q})$, and a time-dependent part, $b(t)$, is found to be a good approximation during a one-dimensional (1D) collapse. The spatial perturbation is assumed to be of the potential type, $\psi = \nabla_q \varphi$, with no rotation. The function $b(t)$ characterizes the growing amplitude of the perturbation in the growing mode. On requiring mass-conservation and Poisson equation, one obtains from the zeroth-order equation and the conventional rate of change of the universal, dimensionless, length scale $a(t)$, and from the first-order equation an approximate expression for $b(t)$:

$$b \propto [1 + 2.5\Omega_0 z/(1 + 1.5\Omega_0)]^{-1}, \tag{2}$$

where Ω_0 is the present universal density parameter and z is the cosmological redshift. This expression reduces to the familiar linear growth rate in an $\Omega_0 = 1$ universe, $b \propto t^{2/3}$, and it approaches a constant in an open universe after $1 + z \sim \Omega_0^{-1}$. The velocity of each particle is

derived from equation (1) to be

$$\dot{\boldsymbol{r}} = (\dot{a}/a)\boldsymbol{r} - a\dot{b}\psi(\boldsymbol{q}), \tag{3}$$

in which the first term corresponds to the Hubble flow and the second term describes the peculiar velocity (which does not exist in an isothermal perturbation). The local density at the neighborhood of each particle is given by the reciprocal of the Jacobian

$$\rho(\boldsymbol{q}, t) \propto [\det(\partial \boldsymbol{r}/\partial \boldsymbol{q})]^{-1}, \tag{4}$$

which is related to the deformation tensor $d_{ij} = \partial^2\varphi/(\partial q_i \partial q_j)$ via $\partial r_i/\partial q_j = a(\delta_{ij} - b\, d_{ij})$. The assumption of a shear perturbation with no rotation implies that the deformation tensor is symmetric and therefore can be diagonalized with principal axes $\hat{q}_i$, $i = 1,3$. In the diagonalizing coordinates one obtains

$$\rho(\boldsymbol{q}, t) = \bar{\rho}(t)[1 - b(t)\lambda_1(\boldsymbol{q})]^{-1} \times [1 - b(t)\lambda_2(\boldsymbol{q})]^{-1}[1 - b(t)\lambda_3(\boldsymbol{q})]^{-1}, \tag{5}$$

where $\bar{\rho}$ is the mean density in the universe, and $\lambda_i(\boldsymbol{q}) \equiv \partial^2\varphi/\partial q_i^2$ are the eigenvalues. A positive λ_i corresponds to an eventual collapse in the ith direction. Assume $\lambda_1 \leqslant \lambda_2 \leqslant \lambda_3$. If λ_3 is positive and has a local maximum $\lambda_{3,\max}$ at some particle, the local density at this particle grows to infinity at a finite time t_c defined by $1 - b(t_c)\lambda_{3,\max} = 0$. This is due to intersection of trajectories of neighboring particles along the q_3 axis. The time t_c is referred to as the moment of *caustic* formation, or *focusing*. If $\lambda_2 < \lambda_3$, the perturbation along the other two axes is still finite at t_c. If the eigenvalues are indeed correlated over the coherence length of the perturbation, one expects the formation of a planar structure on that scale, normal to the r_3 axis, which can be expanding, or contracting more slowly, along the orthogonal axes. It is highly probable that λ_3 is indeed large enough relative to λ_2 and λ_1 so that the collapse would be essentially one-dimensional (Doroshkevich 1970; see § VI). The density profile at early stages is then $\delta\rho/\rho \approx b(t)\lambda_3(q_3)$.

b) *Adiabatic Invariants*

After a particle crosses the plane, it goes on oscillating about it in the r_3 direction, which we refer to as Z hereafter. We would like to estimate how the amplitude of this oscillation, Z_m, changes in time due to the expansion in the orthogonal directions. When the period of oscillation, T, becomes small in comparison with the time scale associated with the expansion, there is an adiabatic invariant given by

$$\int_0^T \dot{Z}^2\, dt \approx \text{const.}, \tag{6}$$

which can guide us to a rough estimate.

In order to calculate it, let us assume for simplicity that the system is symmetric such that $\rho(r) = \rho(|Z|)$. The gravitational field is directed toward the plane and is given by

$$\mu(Z) = \pm 2\pi G \int_{-Z}^{Z} \rho(Z)\, dZ. \tag{7}$$

A simple scaling argument is as follows: if h, v, and μ are some mean values of Z, $\dot{Z}$, and $\mu(Z)$ at a time t, equation (6) requires that $v^2 T \sim$ const.; i.e., $hv \sim$ const. because $T \sim h/v$. Since $v \sim \mu T$, the thickness is expected to behave in time like

$$h \propto \mu^{-1/3} \propto R^{2/3}, \tag{8}$$

where R is the length scale in the plane. When the pancake expands, it becomes thicker, but the relative flattening ($\sim h/R$) becomes more pronounced.

More precisely, consider now two simple limiting cases for the distribution of matter in the region $|Z| < |Z_m|$ that creates the potential well under which our test particle oscillates.

i) The matter is concentrated in a thin disk: $\rho(Z) = \sigma\delta_{\text{Dirac}}(Z)$. In that approximation the field is constant in each side of the plane, i.e., $\mu = \pm 2\pi\sigma$. The maximal velocity and the period of oscillation are related to Z_m via $\dot{Z}(Z = 0) = (-2\mu Z_m)^{1/2}$ and $T = 4(-2Z_m/\mu)^{1/2}$, and the adiabatic invariant is

$$\text{const.} = \int_0^T [\dot{Z}(0) + \mu t]^2\, dt \propto Z_m^{3/2}\sigma^{1/2}. \tag{9}$$

The surface density, σ, varies in time like

$$\sigma(t) \propto R(t)^{-2} M(Z_m, t), \tag{10}$$

where $M(Z_m, t)$ is the mass in the region $|Z| < |Z_m|$, which varies during the gradual collapse due to mixing of layers. Hence, the height scale varies like

$$Z_m(t) \propto R(t)^{2/3} M(Z_m, t)^{-1/3}. \tag{11}$$

ii) The matter is spread in a homogeneous cylinder: $\rho(Z) = \text{const.}$ Here the gravitational field $\mu(Z) = \pm 4\pi G\rho Z$ induces a motion of a harmonic oscillator with an angular frequency $\omega = (4\pi G\rho)^{1/2}$. The adiabatic invariant is then

$$\text{const.} = \int_0^T (Z_m\omega \cos\omega t)^2\, dt \propto Z_m^2\rho^{1/2}. \tag{12}$$

The density ρ varies in this case like

$$\rho(t) \propto R(t)^{-2} Z_m(t)^{-1} M(Z_m, t), \quad (13)$$

so that again, as in the previous case,

$$Z_m(t) \propto R(t)^{2/3} M(Z_m, t)^{-1/3}. \quad (14)$$

At some stage after t_c we expect the above approximation to hold, and $M(Z)$ to reach a constant asymptotic value. Thus, as long as the pancake expands, the axial ratio is expected to decrease slowly in proportion to

$$Z_m(t)/R(t) \propto R(t)^{-1/3}. \quad (15)$$

If the expansion in the pancake plane is unperturbed, one has $R(t) \propto a(t)$, which reduces to $R(t) \propto t^{2/3}$ in an Einstein–de Sitter universe, such that $Z_m/R \propto t^{-2/9}$. We shall come back to this approximation in § V, after presenting the numerical experiment and results.

The estimate (15), which explains the long-lived flattening that shows up in the N-body system when it is "observed" in a cosmologically expanding frame of reference (see Fig. 1 below), gives the illusion that the Z velocities have been suppressed by some fictitious dissipation. Indeed, if $\eta = r/a$ is the position of a particle in the expanding frame, the acceleration in this frame, $\ddot{\eta}$, has a cosmological drag term, $-2\dot{a}/a\eta$, which tends to suppress the peculiar velocity, i.e., make the particle comove with the general Hubble expansion at some new position. In the case of a one-dimensional adiabatic perturbation, this drag acts preferentially along the Z direction, where the peculiar velocities are substantial. Because of the fact that the initial peculiar velocities point toward the X-Y plane, the particles eventually settle down closer to it.

III. THE NUMERICAL EXPERIMENT

a) The N-Body Code

The N-body code is based on the integrator developed and kindly made available to us by Aarseth (1972). It integrates the equations of motion of N particles which interact via the softened Newtonian potential

$$\varphi_{ij} = -Gm_i m_j / \left[(r_i - r_j)^2 + \varepsilon\right]^{1/2}, \quad (16)$$

in which m_i and r_i are the mass and the position of the ith particle and ε is the softening parameter. A fourth order polynomial predictor-corrector method is combined with the scheme developed by Ahmad and Cohen (1973) for the separate treatment of the force field due to nearby and to distant particles. A detailed description of the integration method can be found in the two references mentioned above.

N is less than 1000 in our experiments. If we want each particle to represent a tightly bound galactic-size object in a SC of less than 1000 members, the softening parameter imitates the effect of the finite spatial dimensions of the interacting objects in penetrating collisions, and should therefore be relatively small. On the other hand, when using less than 1000 particles to simulate the evolution of a physical system with many more particles (e.g., massive neutrinos), substantial softening is essential in order to suppress the artificial two-body relaxation effects that arise in the experiment due to the small number of particles. The softening parameter in that case should be at least of the order of the mean distance between nearest neighbors (see a discussion of two-body relaxation under a softened potential in White 1978, and references therein).

The units of the experiment are defined such that $G = 1$, the time unit is t_c, and the length unit is $l_c/18$, where l_c is the critical damping length scale at $t = t_c$ (l_c is the radius of an unperturbed expanding sphere encompassing the critical damping mass). We have tried values of ε in the range $0.5 \leqslant \varepsilon \leqslant 2$. For $N = 250$ and $\varepsilon = 2$ the two-body relaxation is unimportant until $t \sim 10t_c$.

Integration time steps were chosen so that the range of variation of the total energy of the system over t_c was less than 1% of its absolute value. The experiment was run on the VAX of the Physics department at Caltech, where the first collapse of a 250-body system lasted 5–10 minutes of computer time.

b) Initial Conditions

We start with a small-amplitude, adiabatic perturbation, originally inside a spherical volume of the critical damping scale, which is embedded in an Einstein–de Sitter universe. We have in equation (1)

$$a(\tau) = b(\tau) = \tau^{2/3}, \quad \tau \equiv t/t_c, \quad (17)$$

where the units are chosen such that $a(1) = b(1) = 1$, and the Hubble constant is $H(\tau) \equiv \dot{a}/a = 2/(3\tau)$.

We consider a first-order perturbation of the form

$$\psi_i(q_i) = \Lambda_i (l_c/\pi) \sin(\pi q_i / l_c), \quad i = 1,2,3, \quad (18)$$

for comoving coordinates in the range

$$-l_c \leqslant q_i \leqslant l_c. \quad (19)$$

Perturbations on other scales are ignored at the initial stage (note that similar initial conditions were assumed by Doroshkevich *et al.* 1980). The three parameters $\Lambda_1 \leqslant \Lambda_2 \leqslant \Lambda_3$ determine the perturbations along the three principal axes. They coincide with the eigenvalues $\lambda_i(q_i)$

of the deformation tensor for $q_i = 0$. Their ratios determine the asphericity of the perturbation, while their absolute values just scale the times of collapse. We chose $\Lambda_3 = 1$ for the Z perturbation, and try two alternatives in the plane: an unperturbed case with $\Lambda_1 = \Lambda_2 = 0$, and a slightly bound case with $\Lambda_1 = \Lambda_2 = 0.125$. In both cases t_c is much smaller than the mean crossing time in the plane.

On defining $Q_i \equiv \pi q_i / l_c$, one finds in equation (1) that for $\tau < 1$ the perturbation evolves according to

$$r_i(\tau) = (l_c/\pi)\tau^{2/3}\left(Q_i - \Lambda_i \tau^{2/3} \sin Q_i\right), \quad (20)$$

and according to equation (3) the velocity field varies as

$$\dot{r}_i(\tau) = 2/(3\tau)\left[r_3(\tau) - \Lambda_i (l_c/\pi)\tau^{4/3} \sin Q_i\right]. \quad (21)$$

The initial density perturbation has the quite general shape $\delta\rho/\rho = \Lambda_3 \tau^{2/3} \cos Q_3$ for $-\pi \leqslant Q_3 \leqslant \pi$.

We follow the perturbation analytically until $\tau_{\rm in} = 0.25$ ($a_{\rm in} \approx 0.4$), when the numerical simulation starts. N identical particles are distributed homogeneously in a sphere of a comoving radius $q = l_c$. Their comoving positions are determined at random or, alternatively in some cases, on a cubic grid in order to suppress Poissonian clustering on small scales. The initial perturbation at $\tau_{\rm in}$ is set by perturbing the positions and the velocities according to equations (20) and (21).

In an $\Omega = 1$ universe the mass of the system should be

$$M = (4\pi/3)\rho_{\rm crit}(t)\left[a(t) l_c\right]^3, \quad (22)$$

where $\rho_{\rm crit}(t) \equiv 3H(t)^2/(8\pi G)$ is the critical density at time t. In the units of the experiment we have $m = 2l_c^3/9$. We choose arbitrarily $l_c = 18$ and have $M = 1296$. The mass unit of the experiment corresponds to

$$\tilde{m} = 4.82\ 10^{12}\ M_\odot h^2 l_{18}^3, \quad (23)$$

where $l_{18} \equiv a_0 l_c/18$ Mpc corresponds to the comoving damping length scale normalized to the present.

Various cases were simulated, in which the initial parameters were chosen as in Table 1. The situation $\lambda_1, \lambda_2 \ll \lambda_3$ is highly probable (see § VI), and was therefore chosen to be our standard study case with $\Lambda_1 = \Lambda_2 = 0$, $\Lambda_3 = 1$. Exceptions are cases N, O, and P that were constructed to resemble the observed deviation from a Hubble expansion in the plane of the LSC (cf. Aaronson *et al.* 1982 and references therein), in which the systematic infall velocity at the Local Group toward Virgo (in comoving coordinates), v_p, is between 0.1 and 0.5 of the Hubble velocity there, $v_{\rm H}$. In those cases one has at the edge of the disk $v_p/v_{\rm H} \approx 0.1, 0.5$ at $\tau = 1, 5$, respectively, and at the half mass radius $v_p/v_{\rm H} \approx 0.2, 0.8$, respectively. Case O had initially an additional density perturbation of 6% of the mass spread at random inside the central 0.17 l_c radius sphere, which was introduced in order to cause the formation of a rich cluster at the center of the SC, à la the Virgo Cluster in the LSC. For the purpose of the present paper we mostly make use of case M, which has 500 particles and an initial Poissonian spectrum of subfluctuations. We find that the variations of the initial conditions have only marginal effects on the eventual global shape in the cases studied, so that case M can indeed serve here as a study case.

The various cases were followed till $\tau = 5$ or $\tau = 10$. The positions and the velocities of the particles were recorded every $\Delta\tau = 0.25$, where checks for numerical errors were done. These data are later analyzed.

c) *A Dissipative Pancake in a Nondissipative Halo*

The N-body system as a whole provides a natural tool for the study of the nondissipative scenario of SC formation. We can use the same simulations, however, to study the dissipative model as well, because after galaxies are formed as discrete objects in a thin pancake, the overall dynamics becomes dissipationless. One should carefully choose the initial conditions for the pancake galaxies right after their formation, and let them evolve as an N-body system which is embedded in an N-body halo (neutrinos?). Technically, we simply identify the

TABLE 1

INITIAL CONDITIONS

Model	N	ε	Distribution	Λ_1	Λ_2	Λ_3	$\tau_{\rm end}$
J	250	1	random	0	0	1	10
K	250	2	random	0	0	1	5
L	250	0.5	random	0	0	1	2.25
M	500	2	random	0	0	1	5
N	250	2	random	0.125	0.125	1	5
O	250	2	grid + core	0.125	0.125	1	5
P	250	2	grid	0.125	0.125	1	5
R	250	2	grid	0	0	1	10

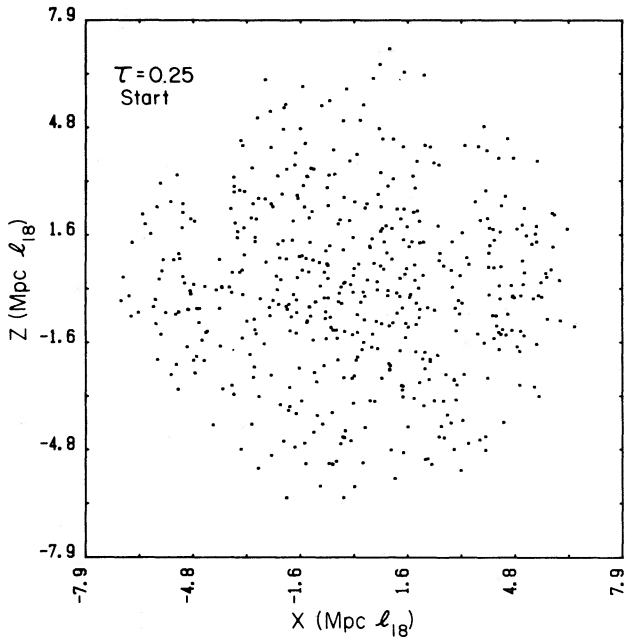

FIG. 1a

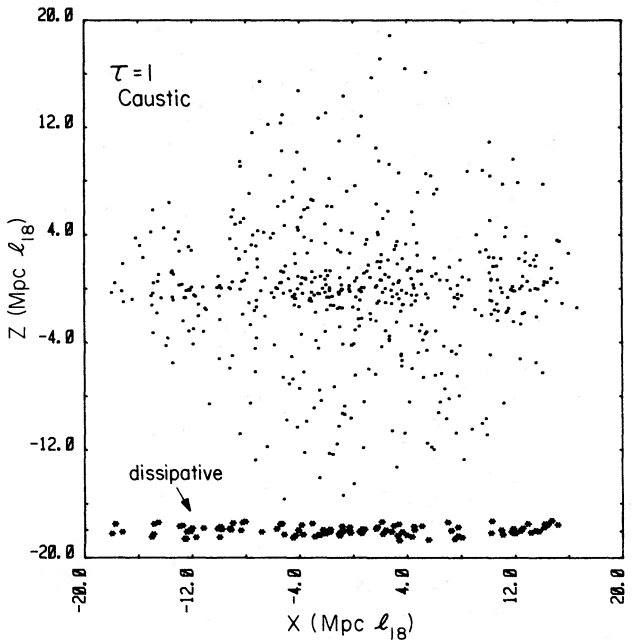

FIG. 1b

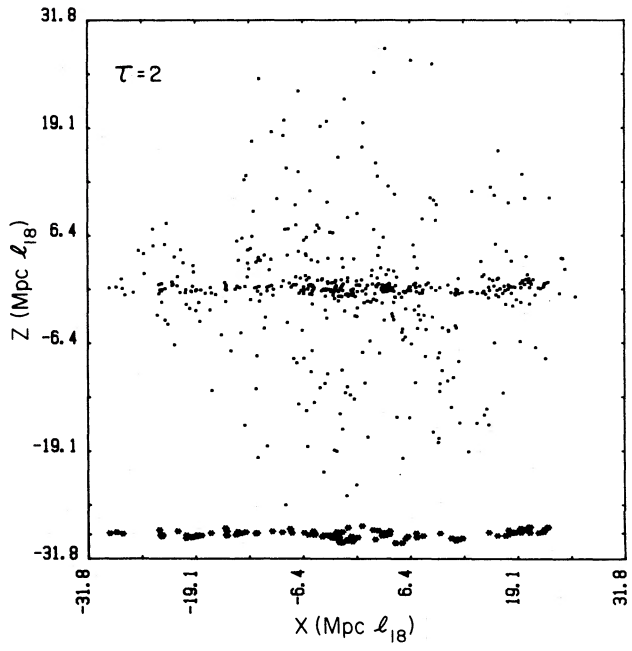

FIG. 1c

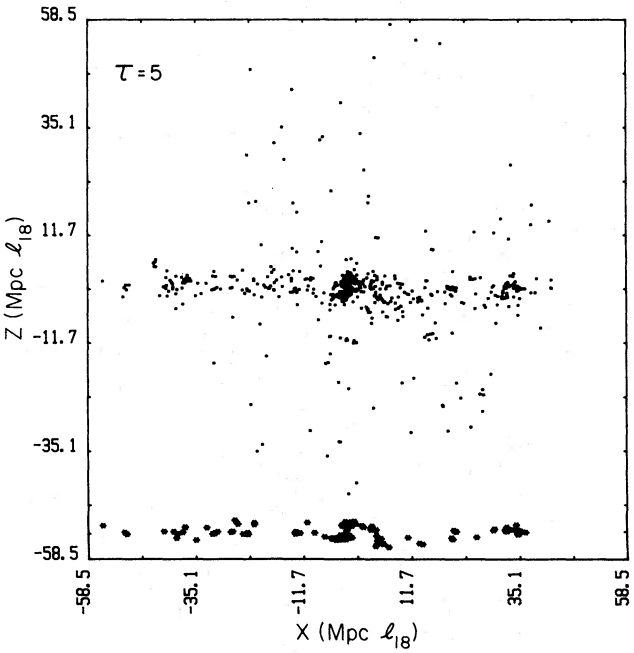

FIG. 1d

FIG. 1.—Edge-on and face-on snapshots of case M at various stages of evolution. The plots are comoving with the Hubble flow. Units are those of the experiment. The 20% "dissipative" pancake is displaced to the bottom (*).

20% particles which have the minimal values of $|r_3|+|\dot{r}_3|$ at $\tau = 1$, and refer to them as dissipative pancake particles thereafter. Their evolution is studied separately and compared to the evolution of the system as a whole. The dissipative pancake initial conditions that are set in this way are somewhat arbitrary; the actual degree of gas dissipation associated with the collapse and galaxy formation, and hence the initial thinness of the pancake and its Z velocity dispersion, at $\tau = 1$, are unknown *a priori*. By defining the pancake as above we just pick up an illustrative example which corresponds to substantial dissipation.

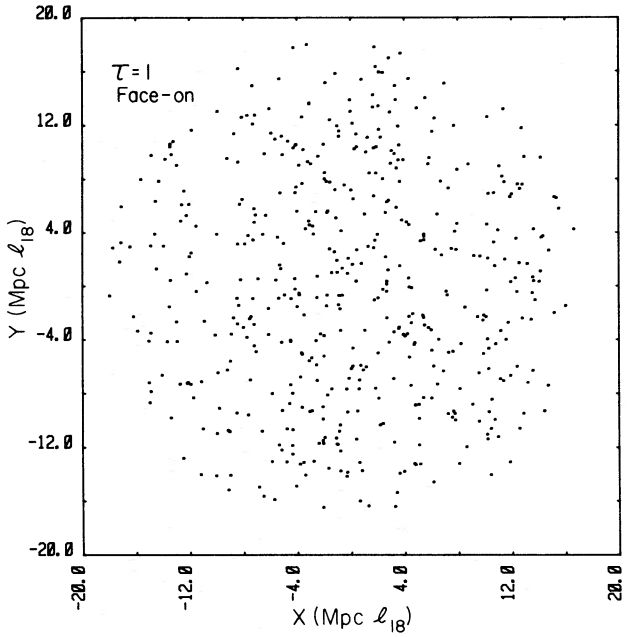

FIG. 1e

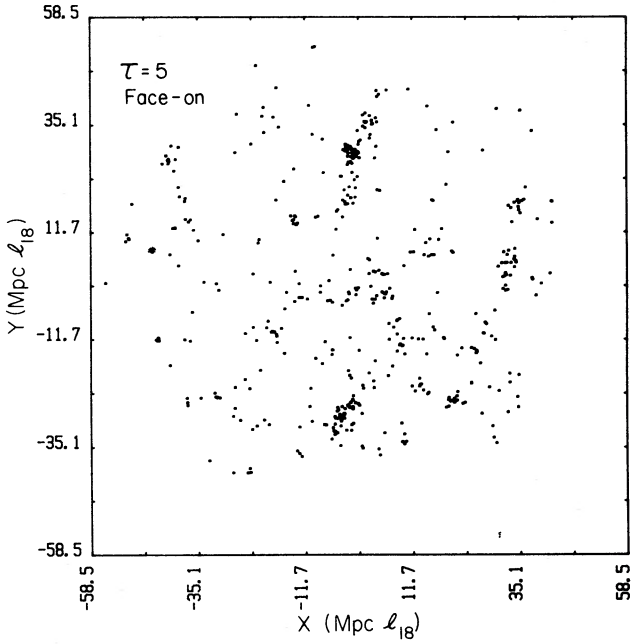

FIG. 1f

IV. FLATTENING IN THE NUMERICAL EXPERIMENT

Edge-on and face-on projections of model M at various time stages are shown in Figure 1 in cosmologically comoving coordinates. Slight flattening is already visible at $\tau = 0.25$. At $\tau = 1$, when about 20% of the particles have collapsed to the plane, the "galaxies" of the dissipative pancake are identified and marked by an asterisk. The dissipative component is displaced from the center to the bottom of the picture. The subsequent snapshots illustrate the remarkable flattening of the system (even with no dissipation!) as it expands in the plane. Note that the absolute thickness of the pancake grows after the first collapse, as is expected from a nondissipative system. It is the relative flattening (i.e., the axial ratio) that becomes more and more pronounced.

Local clustering develops on a time scale which depends on the model parameters. Two rich clusters and several groups develop in case M, in a qualitative similarity to known SCs. At late stages, the sizes of the rich clusters may become comparable to the thickness of the pancake so that they affect the global flattening.

a) A Comparison with the LSC

i) *Flattening by Latitude*

First, we measure the flattening in our N-body systems according to the method used by Yahil, Sandage, and Tammann (1980 [hereafter YST], their Fig. 13) for the LSC. "Galaxies" are counted in bins of $\Delta \sin \beta = 0.05$, where β is the latitude as measured from the center of the SC. YST sample of bright galaxies (~ 13th mag) is based on the *Revised Shapley-Ames Catalog* (Sandage and Tammann 1981). Based on the low, mean peculiar velocities in the LSC (see also Rivolo and Yahil 1982; Tully 1982, in support of this assumption), they were able to deduce the approximate three-dimensional positions of the galaxies, directly from their redshifts, on assuming a pure Hubble flow and excluding galaxies with high peculiar velocities in the 6° core of the Virgo cluster (87 galaxies) and in Fornax (13 galaxies). The sample which is analyzed in their Figure 13 contains the 416 galaxies with Virgocentric velocities of less than 1000 km s^{-1}, which is the typical radius of the flat configuration in the LSC.

The N-body system is analyzed in a similar way, and the corresponding histograms are shown in Figure 2 (*solid lines*) at various time stages. They are normalized to the total number of 416 particles in YST. The possible dissipative pancake component is shown at late stages (*shadowed area*). The observed histogram of YST is shown in the background for comparison (*dashed line*). The N-body system itself develops a bicomponent structure which is typical of most SCs (cf. Tully 1982): a thin, condensed sheet and an extended, dilute halo. This structure is formed with no dissipation, and is preserved for a long time. Even if one adds (unrealistically) all the 100 excluded galaxies of the Virgo core and Fornax to the central bin of YST, it is clear that after $\tau = 1$, the flattening of the simulated system becomes more pronounced than that of the observed SC. The nondissipa-

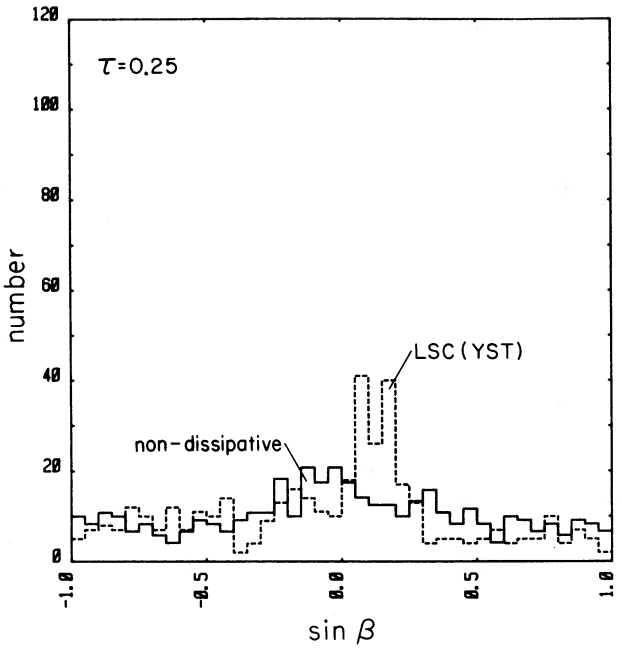

FIG. 2a

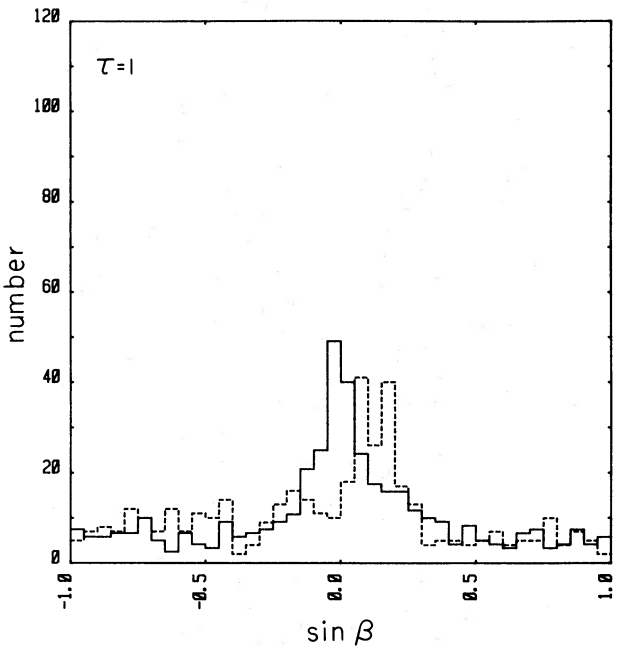

FIG. 2b

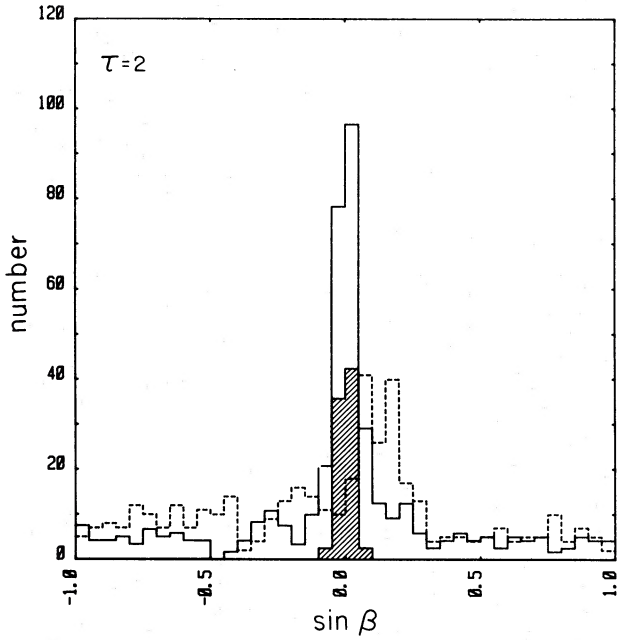

FIG. 2c

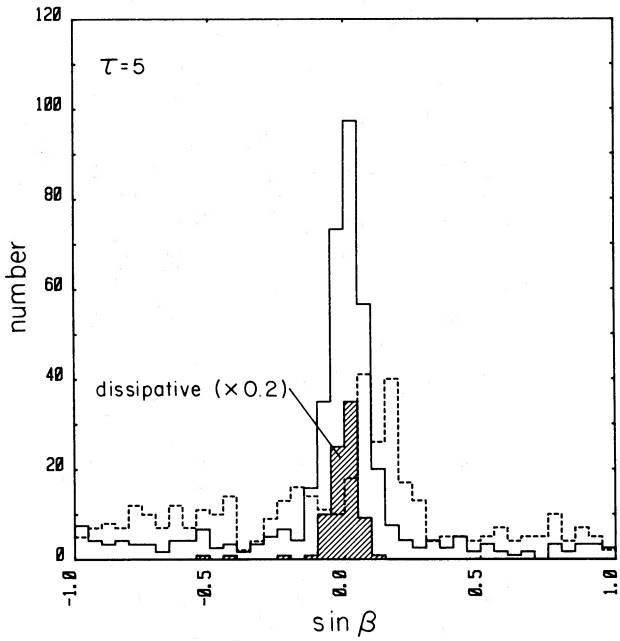

FIG. 2d

FIG. 2.—Counts of particles in latitude intervals as measured from the center of the SC at various time stages (*solid line*). The counts of YST in the LSC are shown for comparison (*dashed line*).

tive histogram seems to be comparable to the observed one near $\tau = 1$, but the dissipative pancake is always much flatter (at $\tau = 5$, the central bin of the pancake would contain 300 galaxies by itself when normalized to 416 total!).

A simple parameter that quantifies the flattening is the half-width of a normal curve that is fitted to the histogram. i.e, the latitude $\bar{\beta}$ that encompasses 68% of the mass. This parameter has a value of $\sin\bar{\beta} \approx 0.5$ in Figure 13 of YST, and it reduces to $\sin\bar{\beta} \approx 0.4$ if the Virgo core and Fornax are added to the central bin. The values of $\sin\bar{\beta}$ in four of the numerical experiments are shown in Figure 4*a* as a function of the expansion parameter a. They are evaluated separately for the nondissipative system as a whole and for the dissipative pancake. The flattening of the nondissipative system resembles YST between $0.5 < a < 1$, i.e., slightly before the first caustic forms. It drops below the observed value at later times. No significant difference shows up between the global flattening of the different cases—for example, neither the strength of local interactions and the degree of clustering (compare cases R, M, J) nor the small peculiar infall velocity in the LSC (case N) has an important effect on the above conclusion. On the other hand, local clustering enhances the thickness of the originally very thin dissipative pancake (compare J and N with M and R), but it never grows above $\sin\bar{\beta} = 0.1$. As a prediction for the dissipative theory we can specify that the flattening, $\sin\bar{\beta}$, of the pancake relative to that of the halo is typically 0.025 before local clustering becomes important, but it finally grows above 0.05 due to strong clustering.

In order to make a more realistic comparison, one should take into account the fact that the flat component of the LSC is not as perfect a plane as our simulated one. Tully (1982) estimates, however, that the local thickness is roughly two-thirds of the global thickness, so that the warping of the pancake is not too large. Hence, our numerical flattening should be modified only by a factor smaller than 1.5. Our qualitative conclusion would not be affected, but the range for the preferred age of the LSC would become $1 \leqslant a \leqslant 1.5$.

Another complication is due to the fact that the count of galaxies in latitude bins is affected by the density profile along the plane. The LSC has the Virgo Cluster as a density enhancement at its center (approx. 20% in mass)—a feature that is not pronounced in the simulated system except in case O. The resultant steeper density gradient in the LSC may be responsible for some smearing of the peak in the latitude histogram of YST. The alternative measure of flattening which is discussed next is not directly affected by that density gradient along the plane.

ii) *Flattening by Parallel Layers*

Here, we measure the flattening in a way which is comparable to that used by Tully (1982, Fig. 4) in his detailed study of the shape of the LSC which is based on the Atlas and Catalog of Nearby Galaxies (Tully and Fisher 1982). Tully, like YST, has reproduced the three-dimensional distribution of galaxies directly from their redshifts, on assuming low-velocity dispersion out of the 6° radius core of the Virgo Cluster. Galaxies are counted in layers of constant thickness ΔZ, which are parallel to the plane of the supercluster. The histogram in his Figure 4 is based on those galaxies in the catalog which are brighter than -18 mag $+ 5 \log h$, and are confined by the Cartesian SC coordinates (in Mpc h^{-1}) $|\mathrm{SGX}| < 10$; $0 < \mathrm{SGY} < 15$ (where the Milky Way is at the origin and the center of the Virgo Cluster is roughly at $-2.6; 10.7; -0.4$). There are 334 such galaxies inside $|\mathrm{SGZ}| < 10$, but the 62 galaxies in the 6° radius core of the Virgo cluster are excluded from his histogram. For the comparison with our numerical results we add them in Figure 3 (*dashed line*) to the four bins centered on $\mathrm{SGZ} = -0.5$ (24 galaxies to each of the two inner bins, and 7 to each of the two outer bins).

The corresponding histograms that describe the flattening of our N-body system in various stages of evolution are shown in Figure 3 (*solid lines*). Recall that the length unit of the experiment, $\tilde{l}$, corresponds to 1 Mpc $l_c/18$ Mpc, where $a_{\mathrm{in}} l_c$ is the initial radius of the system at $a_{\mathrm{in}} = \tau_{\mathrm{in}}^{2/3}$. The present radius of the flat component of the LSC is roughly 10 Mpc h^{-1} (cf. YST). If we assume an unperturbed Hubble flow in the plane, it indicates that $a_0 l_c \approx 10$ Mpc h^{-1}, so that $\tilde{l} \approx 0.56$ Mpc $h^{-1} a_0^{-1}$ when the experiment is applied to the LSC at present, at a stage of evolution given by a_0. The N-body histograms are here normalized to the total number of 334 galaxies. The 20% dissipative pancake component is shown at late stages (*shadowed area*).

It is evident here, as it was in the fit to YST, that the flattening of the N-body system is comparable to that of the LSC for $a \approx 1$, and becomes much flatter at later stages. This conclusion is not changed if we assume instead a higher value for the unperturbed disk radius $a_0 l_c$ (we have tried $a_0 l_c = 20$ Mpc h^{-1}).

We define the parameter f to be the axial ratio

$$f \equiv Z(68\%)/R, \tag{24}$$

where $Z(68\%)$ is the normal width of the histogram, i.e., the height that encompasses 68% of the mass out to $a_0 l_c$, and R is the radius of the system in the plane ($R = a_0 l_c$ if the plane is unperturbed). Figure 4*b* shows the variation of f with the expansion parameter a. From the histogram of Tully we deduce the values $f = 0.27, 0.21$ for $R = 10, 20$ Mpc h^{-1}, respectively, which are shown in Figure 4*b*. Such values are obtained by the N-body system a little before the caustic formation at $a = 1$. The numerical values of f drop below 0.1 at later stages, and the flattening obtained for the dissipative pancake is again much more pronounced. Thus, our conclusion in favor of the nondissipative scenario is confirmed by the fits to both YST and Tully.

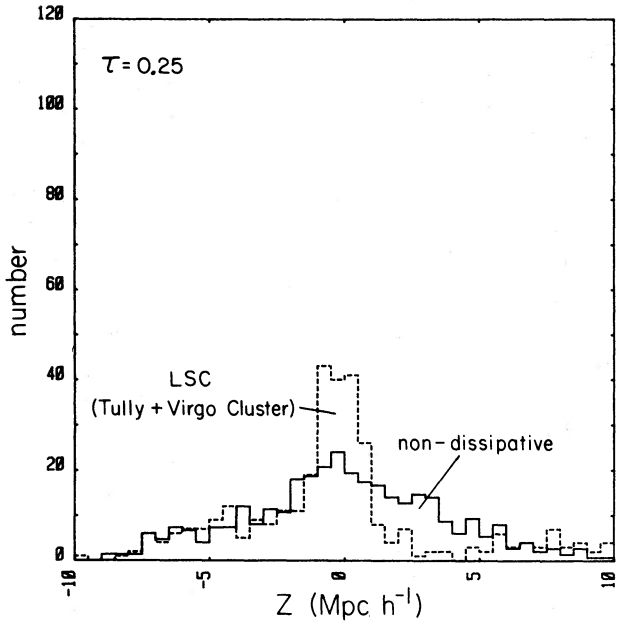

FIG. 3*a*

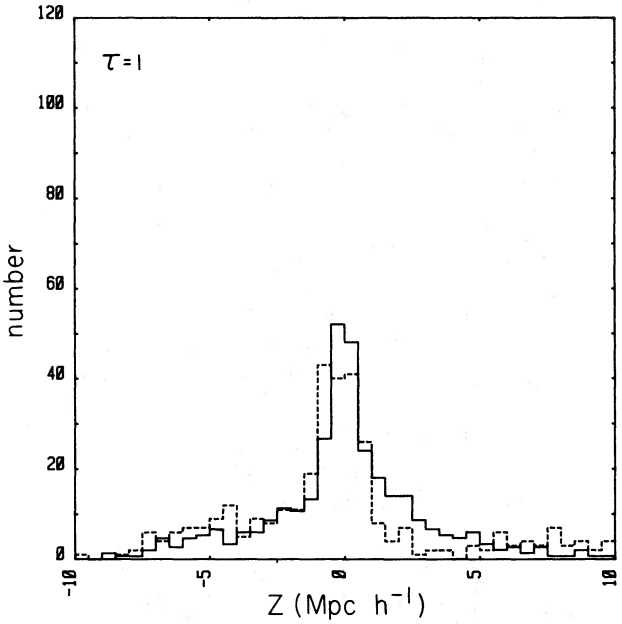

FIG. 3*b*

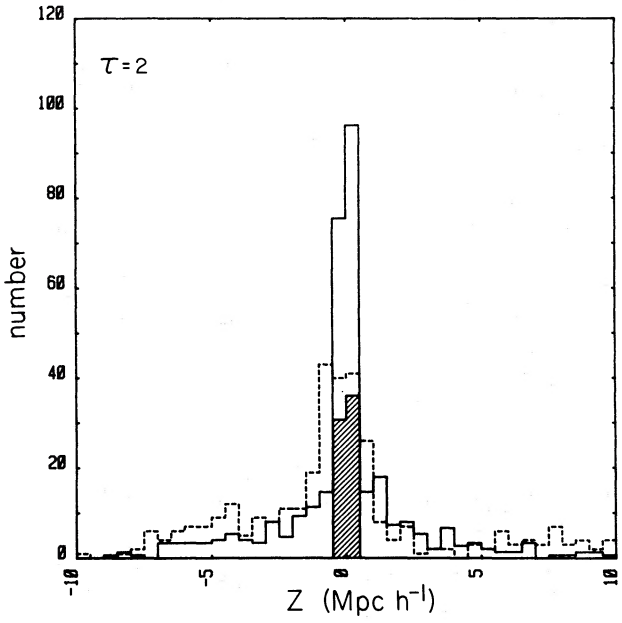

FIG. 3*c*

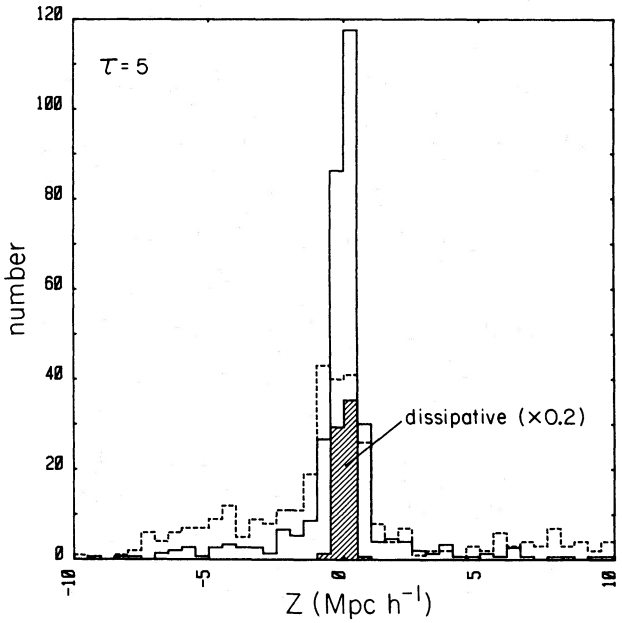

FIG. 3*d*

FIG. 3.—As in Fig. 2, where counts are made in parallel layers, and a comparison is made with the counts of Tully (*dashed line*)

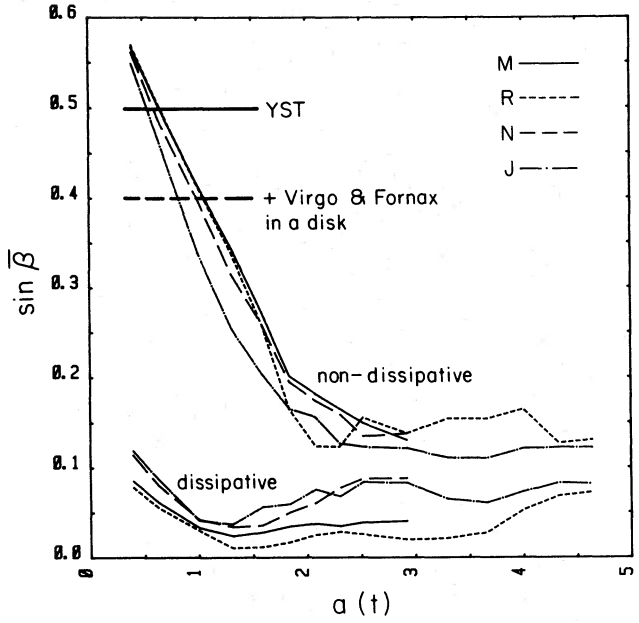

FIG. 4*a*

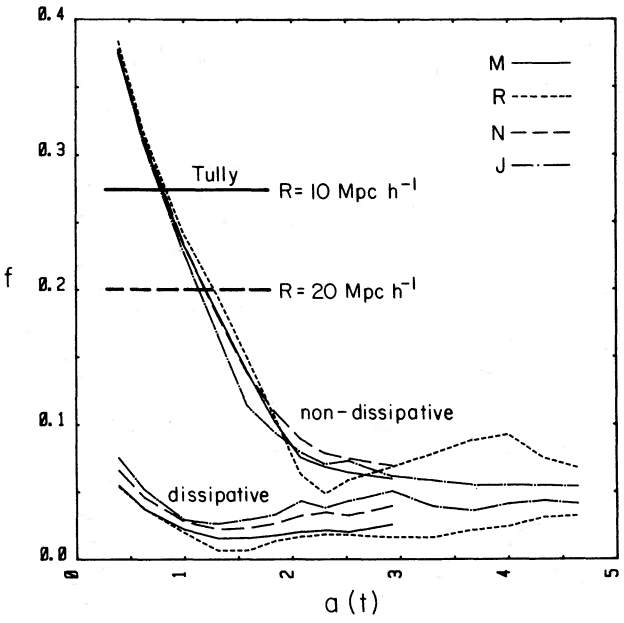

FIG. 4*b*

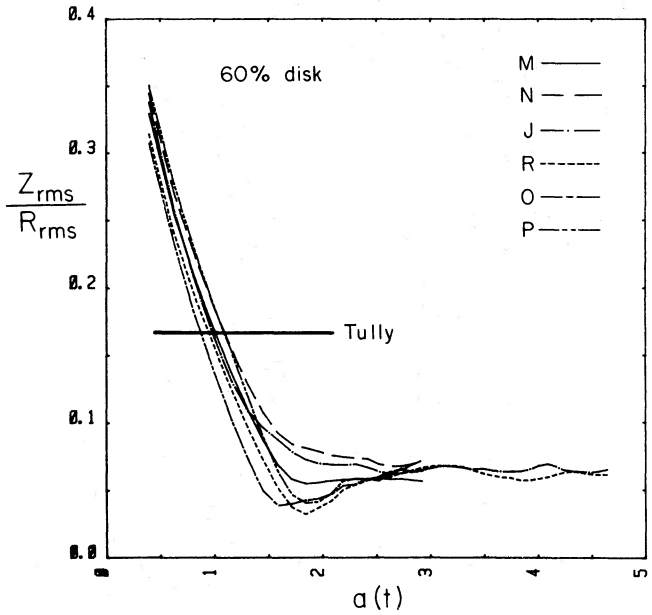

FIG. 4*c*

FIG. 4.—Time evolution of flattening as measured by: (*a*) the latitude $\bar{\beta}$ that encompasses 68% of the particles; (*b*) the axial ratio f that correspond to 68% of the particles; and (*c*) the rms axial ratio of the 60% flat component.

A third possible measure of the flattening may be the rms axial ratio of the system, $f_{\rm rms}$. Tully finds that roughly 60% of the mass in the LSC is confined to a flat component which has an rms axial ratio of 1:6. The axial ratios $f_{\rm rms}$ of the 60% component of our N-body systems are shown in Figure 4*c*. The fit to the observed value is achieved at $a \approx 1$, and the systems maintain a much lower value of $f_{\rm rms} \approx 0.07$ for a long time thereafter.

Here, as in the latitude-bins method, the global flattening is not sensitive to the variation of the parameter values in our different models. In particular, the presence of a dominant cluster at the center of model O, which is included in Figure 4*c*, does not have a significant effect on the axial ratio. (Note that in the grid case, R, $f_{\rm rms}$ drops to ~ 0.04 a little before $a \approx 2$, where the 60% component is at maximum collapse, and only later recovers the value achieved by the other cases. This is a result of the high coherence of the initial perturbation at this case, where in the other cases the field is less regular and local clustering plays some role.)

A modification of the simulated values by a factor of 1.5, trying to account for the warping of the LSC pancake, would not affect our qualitative conclusion, and would bring the preferred age of the LSC to the range $1 \leqslant a \leqslant 1.5$, as before.

It is worth noting that the high central peak of the count in parallel layers is partly due to a radial density gradient. If the Virgocentric number density of galaxies decreases radially like r^{-2} (cf. YST), it contributes a Z gradient of $N(Z) \propto \Delta Z \ln(1 + R^2/Z^2)$ to the number counts in parallel layers of thickness ΔZ and radius R. Hence, although quite flat, the LSC is not as flat as it seems from a first look at Tully's peak.

b) A Comment on External SCs

Quite a few SCs have been identified by now (see Oort 1982), but our knowledge of their detailed spatial

structures is still poor. We make an attempt here to estimate their flattenings from available, incomplete data in a very crude way, but keep in mind that this is not more than an illustration of what should be done when better data become available. This crude estimate is still worth doing in order to get a feeling of how flat the external SCs are in comparison with the LSC, and to make sure that they do not pose a clear stronger requirement on the flattening. The data that have been gathered usually consist of the apparent distribution on the sky of neighboring galaxies or clusters with similar redshifts, and of their radial velocities which are derived directly from the redshifts. The interpretation of the latter is ambiguous because they may reflect either a Hubble expansion, or any other coherent relative expansion or contraction, or even a virialized distribution of velocities, so that their scatter does not give a straightforward indication for the spatial thickness of the SC along the line of sight. We therefore use here only the apparent distribution on the sky, which has a straightforward interpretation.

The apparent axial ratio, f_{ap}, is estimated by eye for the compact, elongated component which usually shows up (probably due to a selection effect where face-on SCs do not show up easily on top of the background). The long axis is determined first, and the short axis is the minimal width that contains a given fraction of the objects in a circle which encompasses the compact component. The estimated values of f_{ap} are given in Table 2, where the number in the next column corresponds to the fraction of objects used to estimate f_{ap}. The estimates of Oort (1982) for the flattenings are given for comparison. The apparent 70% values for Hercules, 1615+43, and 1451+22 are similar, with respect to the roughness of the estimates, to the f-value deduced from Tully for the LSC. Perseus has no halo coverage, so that the estimated value of f_{ap} corresponds to a not-well-defined elongated component which seems to be pretty flat, although still compatible with our nondissipative values of f after the collapse (Fig. 4b). The data on Centaurus-Hydra is too poor for measuring the 70% f_{ap}. Thus, a rough comparison of our theoretical flattening with the observed apparent values is tentatively consistent with the general conclusion from the fit to the better-studied LSC; i.e., a nondissipative scenario can account for the flattening of SCs in general.

When better knowledge of the structure of external SCs becomes available, it may become necessary to consider a variety of initial conditions in the theoretical models, e.g., in order to allow prolate SCs as well. Then one should consider projection effects among other complications in order to make realistic fits. The present stage is much too early for such a detailed study of external SCs.

V. AN APPROXIMATE MODEL

a) In an Einstein–de Sitter Universe

Our intension here is to construct a simple analytical model for the nondissipative evolution, based on the theoretical estimates of § II, that will approximate the results of the numerical experiments for $\Omega_0 = 1$. Such a model will enable us to extrapolate the results to other cases such as an open universe. We assume that each particle behaves according to the formalism of Zel'dovich until it crosses the plane at a time $t_p(\boldsymbol{q})$ that corresponds to $a_p(\boldsymbol{q})$ (the simulations of Doroshkevich *et al.* 1980 indicate that the formalism of Zel'dovich remains a reasonable approximation until roughly 70% of the particles have crossed the plane), and that thereafter it oscillates between $\pm Z_m(a)$ subject to the adiabatic invariant. When averaging over many particles after a_p, we simply consider each particle as if located at the mean height of its oscillation, i.e., $Z = \frac{2}{3} Z_m$ or $Z = (2/\pi) Z_m$ if the gravity is induced, respectively, by a thin disk or by a homogeneous cylinder as in § IIb.

At early stages the height is given by equation (1), i.e.,

$$Z(q_3, a) = (l_c/\pi) a (q_3 - a\psi_3), \qquad (25)$$

TABLE 2

APPARENT FLATTENING OF EXTERNAL SUPERCLUSTERS

SC	Source	Objects	Remarks	(%)	f_{ap}	Oort
Centautus-Hydra ...	Chincarini and Rood 1979, Fig. 3	9 galaxies	...	100	0.2	0.25
Perseus	Gregory *et al.* 1981, Fig. 1	141 galaxies	Compact, elongated component only	...	0.1	...
Coma.....	...	...	...	...	...	0.25
Hercules	Tarenghi *et al.* 1979, Fig. 2	126 galaxies	Elongated component and halo	60 70	0.2 0.3	... ...
1451+22	Ford *et al.* 1981, Fig. 1*a*	17 clusters and groups	...	100 70	0.4 0.25	0.5
1615+43	Ford *et al.* 1981, Fig. 1*b*	11 clusters and groups	...	100 70	0.4 0.15	0.2

until reaching maximum height at an epoch

$$a_m = 0.5 q_3/\psi_3. \tag{26}$$

Later, the particle crosses the plane at

$$a_p = q_3/\psi_3, \tag{27}$$

with a normal velocity

$$\dot{Z}_p = -\tfrac{2}{3} q_3^{1/2} \psi_3^{1/2}. \tag{28}$$

The amplitude of the oscillation at that moment, $Z_{m,p}$, can be evaluated in the two limiting cases discussed above. A lower limit is obtained on considering a maximal infall situation in the thin disk approximation, i.e., on assuming that all the mass is in a disk. This limit is

$$Z_{m,p} = \dot{Z}_p^2/(2\mu_p) = \dot{Z}_p^2/(4\pi G\sigma_p), \tag{29}$$

with the surface density limited by

$$\sigma_p < \rho_p a_p 2 l_c, \tag{30}$$

with ρ_p being the mean density of the universe at a_p. An upper limit is obtained in the homogeneous cylinder approximation with no infall, i.e., on considering only the mass that was originally interior to our test particle. This limit is now similar:

$$Z_{m,p} = \dot{Z}_p/\omega_p = \dot{Z}_p^2(4\pi G\sigma_p), \tag{31}$$

with the effective surface density limited by

$$\sigma_p > \rho_p a_p q_3 \pi/2. \tag{32}$$

Hence, the subsequent evolution of the mean height of each particle, which obeys equations (11) and (14) based on the adiabatic invariant, is limited by equations (29)–(32) to

$$\frac{2}{9}\frac{q_3}{l_c}\frac{q_3^2}{\psi_3}\left(\frac{a}{a_p}\right)^{2/3} < Z(q_3, a) < \frac{8}{3\pi^2}\frac{q_3^2}{\psi_3}\left(\frac{a}{a_p}\right)^{2/3}. \tag{33}$$

Recall that the long, unperturbed axis expands like $R = l_c a$, so that the axial ratio for particles with comoving height smaller than q_3 decreases like

$$\frac{2}{9}\left(\frac{q_3}{l_c}\right)^2\left(\frac{q_3}{\psi_3}\right)^{1/3} a^{-1/3} < \frac{Z(q_3, a)}{R(a)} < \frac{8}{3\pi^2}\frac{q_3}{l_c}\left(\frac{q_3}{\psi_3}\right)^{1/3} a^{-1/3}. \tag{34}$$

The flattening parameter $f \equiv Z(68\%)/R$ is then evaluated on substituting $q_3 = 0.5 l_c$ and choosing $\psi_3 = (l_c/\pi)\sin(\pi q_3/l_c)$ as in the experiment. One obtains

$$0.065 a^{-1/3} < f < 0.157 a^{-1/3}. \tag{35}$$

The model values of f as derived from equation (25) before $a_p(68\%)$, and the limits of equation (35) thereafter, are plotted as dotted lines in Figure 5*a*, in comparison with the results of the numerical experiments.

In order to calculate the latitude flattening parameter, $\bar{\beta}(a)$ in the model, one needs the fraction of mass in latitudes lower than β, i.e.,

$$\tilde{M}(\beta, a) = (l_c 4\pi/3)^{-1}\int_0^{l_c} dq_{12}\, 2\pi q_{12} q_3(q_{12}, \beta, a), \tag{36}$$

where $q_{12} \equiv (q_1^2 + q_2^2)^{1/2}$ is the comoving radius in the plane, and q_3 is the comoving height which corresponds to a latitude β at q_{12}, at an epoch a. The quantity q_3 is obtained by solving numerically the equation

$$\tan\beta = Z(q_3, a), \tag{37}$$

in which the right-hand side is given by equation (25) if $a < a_p$, or by either side of equation (33) if $a \geqslant a_p$. The normal width, $\bar{\beta}(a)$, which is obtained for $\tilde{M}(\bar{\beta}, a) = 0.68$, is plotted in Figure 5*b*, in comparison with the results of the numerical experiments.

Figures 5*a* and 5*b* show a pleasant agreement between the limits obtained by the approximate model and the simulation results in all cases. The simple model is hence found to be a useful approximation which can be applied to other cases as well.

b) In an Open Universe

In Appendix A we calculate $f(a)$ by the approximate model in an open Friedmann universe. The results in the two limiting cases are shown in Figure 6, where no specific value has been assumed for the present value of Ω_0. The cosmological time is expressed alternatively by the expansion parameter a or by the density parameter $\Omega = \Omega_1(1+z)/(1+\Omega_1 z)$, which is normalized arbitrarily to Ω_1 when $a = 1$. Each of the five curves is characterized by its collapse epoch a_c which is given by the value of a at the intersection of the curve with the horizontal line that marks the flattening at t_c (from eq. [A4]):

$$f_c = (q_3 - \psi_3)/l_c. \tag{38}$$

Each curve can alternatively be associated with the amplitude of the perturbation $b(z)$ at some given epoch [e.g., $b_1/(1+\tilde{\Omega}_1 z_r)$, where z_r corresponds to the plasma recombination epoch].

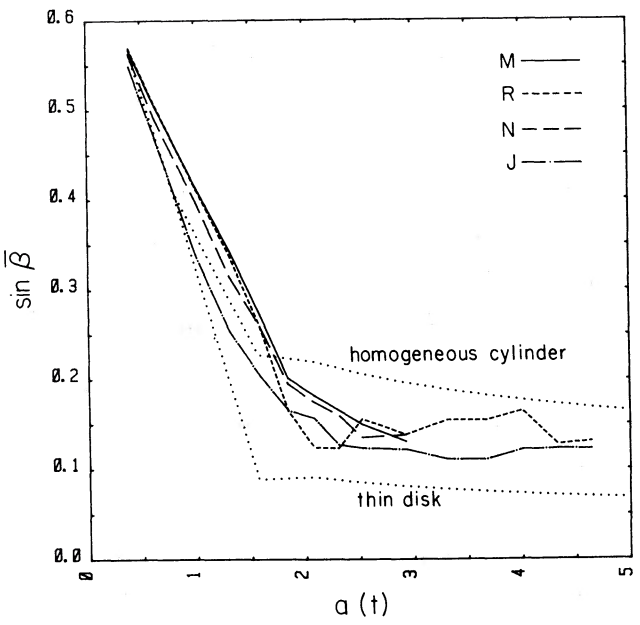

FIG. 5a

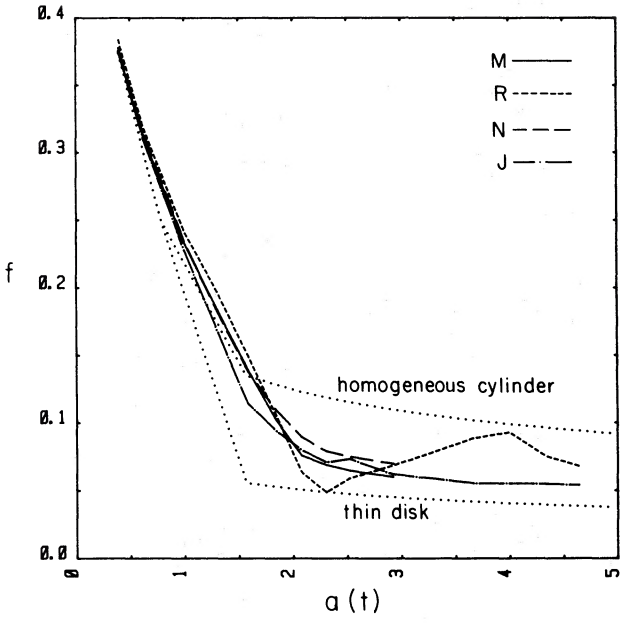

FIG. 5b

FIG. 5.—Limits on the flattenings that are derived by the analytical model are compared with the results of the numerical experiments

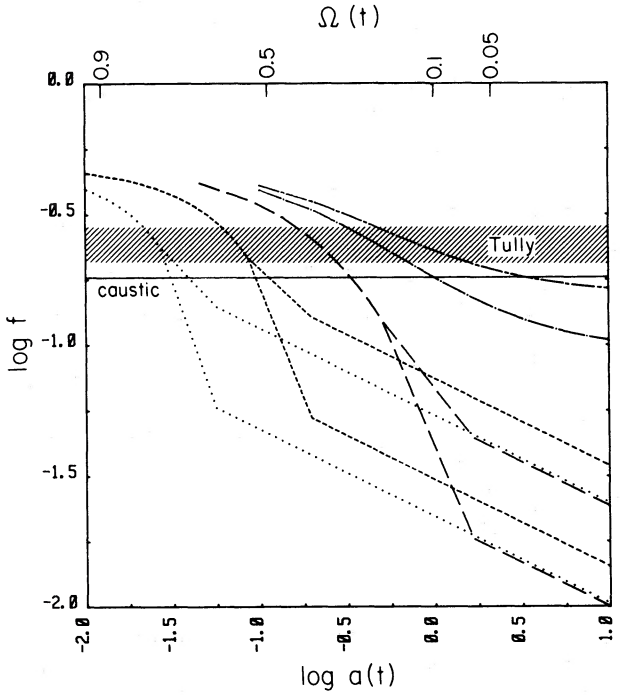

FIG. 6.—Model flattening, f, in an open universe

A way to fit a model to an observed value of flattening, f_o, is as follows: Draw a horizontal line $f = f_o$. Then, for any given value of Ω_0, draw a vertical line $\Omega = \Omega_0$ (i.e., $a = a_0$). A model curve which passes through the intersection point of those lines indicates the fitting model.

The flattening observed by Tully ($f_o \geqslant \frac{1}{6}$) and by YST indicate that $f_o \approx f_c$. Hence, the fitting model is still collapsing near its first caustic formation for any value of Ω_0, where models which are in a later stage of evolution are much flatter. For a smaller value of Ω_0, the observed flattening f_o is obtained by a SC in a slightly earlier stage of evolution; i.e., the present flattening in a given stage of evolution is a little more pronounced if the universe is open, in agreement with the results of White and Silk (1979) and of Doroshkevich *et al.* (1980). Intuitively, this is due to the fact that the pancake expands faster at late stages in an open universe [$a(t) \propto t$ after $1 + z \sim \Omega_0^{-1}$], where unbound perturbations stop growing and are rather "frozen" relative to the rapidly expanding background. It is possible in this case that only part of the proto-SC is bound and has collapsed to a pancake prior to $1 + z \sim \Omega_0^{-1}$, while the rest, now in the SC halo, is expanding with the Hubble flow forever (see Dekel 1982*b*). Thus, the general conclusions which were derived from the numerical experiment in an Einstein–de Sitter universe are valid in an open universe as well. Simulations of superclusters in an open universe are in progress (Aarseth and Dekel 1983).

VI. DISCUSSION

a) *Simplifying Assumptions*

i) *Tidal Interactions*

The system was treated as isolated from its surroundings. It is pretty clear, on the other hand, that the universe is not yet homogeneous on the scale of SCs (cf. Davis, Frenk, and White 1982; Kirshner *et al.* 1981), and therefore mutual tidal interactions between SCs may have some dispersive effects on the individual systems. The fractional change of $\psi(q)$ due to a tidal interaction with a comparable object at a distance d is of the order of ZR^2/d^3. Since we usually expect $Z < R < 2d$, the effect should be small. In particular, there are no obvious neighbors close enough for their tidal fields to have had a strong effect on the LSC.

Binney and Silk (1979) have shown that the resultant shape of systems which were subject to tidal interactions in their linear stage is prolate. Tully (1982) indeed identifies clouds of galaxies in the halo of the LSC that are prolate and point toward the Virgo Cluster—a possible indication for tidal interactions inside the LSC—but the main body of the LSC is oblate, supporting the assumption of no significant tidal interactions with external objects.

Cosmological simulations of a larger region of space that encompass a few SCs would make clear whether or not SCs may be approximated by isolated systems, but it seems to be at least a reasonable first-order approximation.

ii) *Initial Spectrum of Perturbations*

The initial perturbation was assumed to be coherent on the proto-SC scale with no subcondensations apart from the $\sqrt{N}$ Poissonian noise in the random distribution cases. This latter noise, although being quite pronounced in the cases with small N and ε (e.g., J), had no important effect on the final flattening, but it is to be noted that its initial amplitude did not reach that of the global perturbation near the SC scale in any of the models. Hence, the initial spectrum of perturbations is assumed to be truncated below this scale. The adiabatic component is indeed expected to have a sharp cutoff at the critical damping scale (cf. Peebles and Yu 1970; Press and Vishniac 1980; Silk and Wilson 1980; Peebles 1981*b*; and, for the case of massive neutrinos, Bond and Szalay 1981). The isothermal component, which may be responsible for galaxy formation, is assumed here to be still linear near the damping scale when the SC collapses.

This latter assumption is supported by recent measurements (Press and Davis 1981; Kaastra and van Bueren 1981; Bahcall 1981), which indicate that the systematic variation of the present mean density in clusters of galaxies of various richnesses and sizes is small (our interpretation of the two first measurements are that $M \propto R^3$ or $M \propto R^2$, respectively, where M and R are the masses and radii of the clusters). This means that clusters of all sizes, from very small groups to rich clusters, have collapsed at roughly the same epoch, and hence had started as density perturbations of similar amplitudes at recombination. Thus, the contribution of the isothermal component, δ_{is}, to the amplitude of the perturbations on galactic scale ($M_G \sim 10^{12}\ M_\odot$) was not much larger than that of the adiabatic component, δ_{ad}, on SC scale ($M_D \sim 10^{15}\ M_\odot$). If $\delta_{is} \propto M^{-\alpha_{is}}$ ($\alpha = \frac{1}{2} + n/2$, where the power spectrum is $\langle|\delta_k|^2\rangle \propto k^n$) right after the recombination epoch, the observed large-scale fluctuations of the microwave background radiation (dipole and quadrupole) require that (Silk and Wilson 1981) $\alpha_{is} \geqslant \frac{1}{2}$ (or $a_{is} \geqslant \frac{1}{3}$ if the universe is dominated by massive neutrinos), so that $\delta_{is}(M_D) \ll \delta_{ad}(M_D)$ as has been assumed (for more about the possibility of a bicomponent spectrum, see Dekel 1981 and references therein).

The observed dipole in the background radiation indicates for the adiabatic spectrum $\alpha_{ad} \geqslant 1$ (Silk and Wilson 1981), which implies that perturbations on scales larger than M_D do not substantially affect the evolution of $\sim M_D$ SCs (in support of the assumption discussed in § VI*a*[ii] above).

iii) *Likelihood of the Initial Anisotropic Configuration*

Statistical analysis (Doroshkevich 1970; Dekel 1981) has shown that if the initial distribution function of the local density perturbations, $\delta(r)$, is a Gaussian with a width σ, and if the spectrum is truncated at a wavenumber k_D (corresponding to a critical mass M_D), the coherence mass of a perturbation near a density peak with $\delta_0 > \sigma$ is of the order M_D, and it grows with δ_0/σ. If the perturbation was less coherent over the proto-SC, it might have led to a somewhat warped structure, which could increase its apparent thickness; i.e., one should be aware of the possibility that the extreme flattening obtained here may be somewhat due to an overidealized choice of initial conditions. It was mentioned in § IV, however, that the flat component of the LSC seems to be confined to a well-defined plane, the local thickness of which is roughly two-thirds of its global thickness (Tully 1982). Other observed SCs (cf. Einasto, Joeveer, and Saar 1980) also indicate structures which are pretty much planar as the walls of huge cells.

Our basic conclusions are valid for systems in which the initial perturbation in one direction is dominant ($\lambda_3 \gg \lambda_1, \lambda_2$). This is known to be the case in our own LSC (from the small deviation from Hubble expansion in the plane), and would be the case in any SC which is still expanding in two directions. Doroshkevich has shown that the conditioned probability to have the three values $\lambda_3 \geqslant \lambda_2 \geqslant \lambda_1$, given that $\delta/\sigma = \delta_0/\sigma$, is propor-

tional to

$$p(\lambda_1,\lambda_2,\lambda_3) \propto e^{-N(I_1,I_2,\delta_0/\sigma)} \times (\lambda_3-\lambda_2)(\lambda_3-\lambda_1)(\lambda_2-\lambda_1), \quad (39)$$

where $I_1=(\lambda_1+\lambda_2+\lambda_3)/\sigma$ and $I_2=(\lambda_1\lambda_2+\lambda_1\lambda_3+\lambda_2\lambda_3)/\sigma^2$. It means that the probability that two eigenvalues of the deformation tensor will be similar is small. Furthermore, the ratio of the conditioned mean values $\bar{\lambda}_3$ and $\bar{\lambda}_{12}\equiv 0.5(\bar{\lambda}_1+\bar{\lambda}_2)$ is

$$\frac{\bar{\lambda}_3}{\bar{\lambda}_{12}}=\frac{\eta(n)\delta_0+3\sigma/\sqrt{2\pi}}{\eta(n)\delta_0-3\sigma/\sqrt{2\pi}}, \quad \eta(n)=\frac{\sqrt{5}}{3}\left(\frac{n+3}{n+5}\right)^{1/2}, \quad (40)$$

where n is the power index of the spectrum after recombination ($\langle|\delta(k)|^2\rangle \propto k^n$). If $\delta_0 \approx \sigma$ and $n \leqslant 0$, the mean eigenvalue in the plane, $\bar{\lambda}_{12}$, is negative. For any value of n, $\bar{\lambda}_3/\bar{\lambda}_{12}>10$. Thus, for a Gaussian process, the initial conditions assumed here, with $\lambda_3 \gg \lambda_1,\lambda_2$ are highly probable.

Note that the evolution of the proto-SC depends on the ratio λ_3/λ_{12} but not on the absolute value of λ_3. The latter determines the time for the collapse but does not influence the resultant structure; we could therefore choose it arbitrarily to be $\lambda_3=1$, and have initial conditions which were quite general.

Cosmological simulations on larger scales that start from a truncated adiabatic spectrum may tell more about the initial structure of the individual SCs. Two-dimensional simulations (Doroshkevich *et al.* 1980; Melott 1983*b*) have produced a cell structure that seems to confirm the theoretical ideas. Current three-dimensional simulations (Klypin and Shandarin 1982; Davis, Frenk, and White 1982) seem not to show pancakes very clearly, perhaps because of a poor resolution on the relevant scales. More extensive simulations are in progress (Dekel and Aarseth 1983).

iv) *Small-Scale Fluctuations in the Microwave Background*

The isotropy of the microwave background radiation on scales of a few degrees is believed to constrain the possible amplitudes of adiabatic density perturbations at recombination on the scales of SCs. The linear growth rate in the present scenario is similar to that in the conventional gravitational instability picture, i.e., $\delta \propto b(t)$, but here δ on the scale of SCs has reached unity only recently so that the predicted anisotropies are $\delta T/T \approx 2\times 10^{-4}\Omega_0^{-1}$ on scales of a few degrees. The predicted fluctuations are larger in proportion to $1+z_c$, which makes it harder to reconcile early SC collapse scenarios with the observed isotropy of the background on those scales, unless neutrinos dominate the mass in the universe and help reduce the required $\delta T/T$ by a factor of 5–10 (see Doroshkevich *et al.* 1981).

It is still possible, however, that substantial reionization at early epochs (e.g., by a first generation of massive stars; cf. Rees and Kashlinski 1982) and subsequent scattering of the background radiation have erased temperature fluctuations on scales of a few degrees (cf. Peebles 1981*a*). The proposed scenario in which galaxies (or halos) form early, prior to the SC collapse, gives rise to such a possibility.

v) *On the Dissipative Pancake Picture*

The possible interpretation of our numerical experiment as simulating a *dissipative* pancake component in a dominant halo of massive neutrinos should be made with caution, because our choice of initial conditions for the pancake was somewhat arbitrary. The actual thickness of the pancake is sensitive to the detailed dynamics of the shock and thermal processes in the gas (Sunyaev and Zel'dovich 1972; Binney 1972). In fact, neutrinos might have collapsed before the gas (but after they became nonrelativistic at $z\sim 10^4$–10^5), and as a result the gas might not have formed a caustic in the way commonly assumed. Furthermore, the subsequent evolution of a pancake is sensitive to the effectiveness of short-range encounters (see also Aarseth and Binney 1977).

Hence, *one cannot exclude the dissipative scenario* based on the present experiments. A version of this scenario in which galaxies were formed in small pancakes during the large-scale collapse is acceptable. What one may conclude, however, is that—contrary to the common belief—the dissipative scenario is not the *only* scenario that can provide highly flattened pancakes.

b) *Comparison with Results of Others*

An alternative, soluble approximation for the premixing stage is the collapse of a homogeneous ellipsoid (cf. White and Silk 1979). The evolution of our N-body system until t_c is approximated better by the approximation of Zel'dovich, in the sense that the collapse is slower and the flattening near t_c is more pronounced than what is predicted by the homogeneous ellipsoid approximation. The latter breaks down early in the collapse because of a strong density gradient that develops along the collapsing axis. It can still provide an upper limit for the flattening at early stages, which can be matched with our analytical upper limit at later stages.

Related work in the nonlinear regime has been done by Doroshkevich *et al.* (1980) and by Melott (1983*a*) who simulated the evolution of a similar perturbation by means of the "cloud in cell" method in the pure one-dimensional approximation. Doroshkevich *et al.* find

that after the focusing (t_c) the axial ratio of a contracted layer, whose boundaries q_3^* are defined by $\partial r_3/\partial q_3 = 0$, is growing approximately like

$$Z(q_3^*)/R \approx 0.38\left[1-(a_c/a)^{1/2}\right], \qquad (41)$$

when their equation (14) is translated to our notation. For $a \geq a_c$, our simulations and our model estimates also predict a growth of the flattening of the layer inside q_3^* due to the rapid growth of q_3^* in time. When the formalism of Zel'dovich is applied formally to the post-collapse epoch, this growth rate is given by $\cos(\pi q_3^*/l_c) = a_c/a$. If this is a good estimate for q_3^*, however, our results seem not to agree at late stages, when $a \gg a_c$. Then, q_3^* approaches the value $0.5l_c$ that is used by us to define the flattening f, but still their flattening grows asymptotically to a constant ~ 0.38, while our f decreases like $a^{-1/3}$ to smaller values. This discrepancy may be resolved if q_3^* actually grows faster in their simulations, or else it may be due to the fact that their calculations are one-dimensional. Another difference which is probably related to the latter is the multicaustic, multistream configuration which is preserved after the collapse in the one-dimensional simulations but is smeared out in our three-dimensional one because of gravitational scattering.

Aarseth and Binney (1978), and Klypin (1980) have simulated the evolution of N-body systems that started flat but nonexpanding, and therefore ended up with moderate flattening, of the order of 1:2 and 1:3, respectively. These simulations are meant to describe elliptical galaxies or rich clusters and are not relevant to expanding SCs. Nevertheless, they can give some additional insight into the local stellar dynamics.

VII. CONCLUSION

Our main conclusions from the global flattening of SCs are:

1. A nondissipative scenario which starts from an adiabatic perturbation with probable initial conditions can explain the observed flattening of SCs, and no dissipation is required. This means that galaxies could have been formed before the collapse of SCs and not necessarily as a result of that collapse.

2. A fit to the observed flattening of the LSC indicates that it has collapsed in one direction only recently, where 20–50% of the mass has crossed the plane and a caustic has occurred between $z \approx 0.5$ and now. The flattening is expected to be even more pronounced at later stages.

3. A simple analytic model, which is based on the formalism of Zel'dovich before the collapse and on adiabatic invariants afterwards, agrees well with the numerical experiment. It therefore provides a useful tool for studying the nonlinear evolution of flat, expanding systems under various conditions. For example, it has been used here to generalize our conclusions to an open universe.

It may be of interest to mention here some preliminary conclusions concerning other aspects of the dynamics of SCs, which are discussed in associate papers:

a) The Z velocities in the pancake may, in principle, provide important information about the formation of the pancake, on its present stage of evolution, and on Ω_0. Unfortunately, the observed velocities of pancake galaxies (low |SGZ|) are dominated by their fast expansion parallel to the X-Y plane, which makes the measure of the relevant Z velocities possible only for a few nearby galaxies at high |SGB|, and out of the Local Group. We find (Dekel 1983*a*), in a sample of galaxies with redshift-independent measured distances, no evidence for anisotropies in the Virgocentric flow at |SGZ| larger than a few Mpc, and a weak evidence for an infall and excess Z velocities (positive and negative) closer to the plane. This indicates an early stage in the one-dimensional collapse, in agreement with the result obtained from the flattening, and possibly an open universe where the SC halo is "frozen" in the Hubble expansion. The simulations (with $\Omega_0 = 1$) predict for the velocity dispersion in the 60% flat component $\sigma_Z \sim 100$ km s^{-1} at $a \sim 1$, and $\sigma_Z \sim 175$ km s^{-1} at $a \geq 2$, in agreement with the spatial flattening found by Tully (1982) and discussed here.

b) The global overdensity in flat SCs can still be on the order of unity even though much higher densities occur locally. Spherical models and linear approximations, which are commonly applied to SCs in order to derive the mean density in the universe, may lead to spurious results by factors of 1–3 (depending on the age of the SC) because of flattening and nonlinear effects (Dekel 1983*c*).

c) The two-point correlation function within the simulated SC, on scales of a few Mpc, grows in a non–self-similar way as a result of the large-scale collapse to a pancake rather than as a result of local clustering. A power-law $\xi(r) \propto r^{-1.5}$ that agrees with observations in the LSC (Rivolo and Yahil 1981, private communication) is obtained at $a \approx 1.5$ (Dekel 1982, 1983*b*).

d) The clustering of galaxies according to the nondissipative pancake scenario is still very weak at $z > 1.7$, and is compatible with the lack of measurable clustering among the Lyman-alpha absorption systems in quasars (Dekel 1982).

Our basic conclusion is that the present data on the structure and dynamics of the LSC is consistent with a *nondissipative pancake* scenario which is a natural combination of the "eastern" pancake picture and the "western" clustering theory, where both adiabatic and isothermal perturbations play a role in the formation of structure in the universe.

I thank A. Szalay for a collaboration at various stages of this project, and S. J. Aarseth for allowing the use of his code. I am grateful to P. Goldreich for encouragement and advice. It is my pleasure to acknowledge helpful discussions with R. D. Blandford, J. H. Oort, M. J. Rees, A. Rivolo, G. B. Rybicky, J. Silk, S. D. M. White, and A. Yahil. The research was supported in part by the NSF AST80-20005.

APPENDIX A

AN APPROXIMATE MODEL IN AN OPEN UNIVERSE

Our intention here is to calculate $f(a)$ by the approximate model in an open Friedmann universe. The density parameter $\Omega(t)$ is normalized arbitrarily to Ω_1 when the expansion parameter is $a=1$. Each cosmological epoch is then characterized by $1+z=a^{-1}$. According to equation (2) the perturbation grows like

$$b(z)=b_1/(1+\tilde{\Omega}_1 z), \tag{A1}$$

where we have defined for convenience

$$\tilde{\Omega}_1 \equiv 2.5\Omega_1/(1+1.5\Omega_1). \tag{A2}$$

On normalizing as before such that $b=1$ at z_c (caustic formation), we have

$$b_1=1+\tilde{\Omega}_1 z_c. \tag{A3}$$

We now calculate $f(a)$ for a given perturbation which is characterized by its collapse epoch, z_c or a_c.

At early stages the axial ratio is, by equation (1),

$$Z(q_3,a)/R(a)=[q_3-b(a)\psi_3]/l_c, \tag{A4}$$

until maximum height is reached at an epoch

$$z_m=\frac{b_1\psi_3}{\tilde{\Omega}_1 q_3}\left\{1+\left[1-\frac{\tilde{\Omega}_1 q_3}{b_1\psi_3}(\tilde{\Omega}_1^{-1}-1)\right]^{1/2}\right\}-\tilde{\Omega}_1^{-1}. \tag{A5}$$

If the particle is bound, i.e., $b_1>(1-\tilde{\Omega}_1)\psi_3/q_3$, it crosses the plane at

$$a_p=(1+z_p)^{-1}, \quad \text{or} \quad z_p=(b_1\psi_3/q_3-1)/\tilde{\Omega}_1, \tag{A6}$$

with a normal velocity

$$\dot{Z}_p=-H_p(q_3^2/\psi_3)(\tilde{\Omega}_1/b_1), \tag{A7}$$

in which H_p is the Hubble constant at z_p. $Z_{m,p}$ can now be evaluated in the two limiting cases as in the $\Omega_0=1$ case, where here the mean density of the universe at that time is

$$\rho_p=\Omega_1\frac{(1+z_p)}{(1+\Omega_1 z_p)}\frac{3H_p^2}{8\pi G}. \tag{A8}$$

The lower limit obtained for the axial ratio is

$$\frac{Z(q_3,a)}{R(a)}>\frac{2}{9}\left(\frac{q_3}{l_c}\right)^2\left[1-\frac{q_3}{b_1\psi_3}(1-\tilde{\Omega}_1)\right]\left[1+\frac{q_3}{b_1\psi_3}\left(\frac{\tilde{\Omega}_1}{\Omega_1}-1\right)\right]\left(\frac{a}{a_p}\right)^{-1/3}, \tag{A9}$$

and the upper limit is larger by a factor of $12l_c/(\pi^2 q_3)$. The limiting values of f are obtained on substituting

$q_3/l_c = 0.5$ and $q_3/\psi_3 = \pi/2$, as in the experiment. One obtains

$$f > \frac{1}{18}\left[1 - \frac{\pi(1-\tilde{\Omega}_1)}{2b_1}\right]\left[1 + \frac{\pi(\tilde{\Omega}_1/\Omega_1 - 1)}{2b_1}\right]\left(\frac{a}{a_p}\right)^{-1/3}, \quad \text{(A10)}$$

and an upper limit which is larger by a factor of 2.43. Note that expressions (A4)–(A10) reduce to the analogous expressions (25)–(35) in the limit $\Omega_1 \to 1$ ($\tilde{\Omega}_1 \to 1$).

REFERENCES

Aaronson, M., Huchra, J., Mould, J., Schecter, P. L., and Tully, R. B. 1982, *Ap. J.*, **258**, 64.
Aarseth, S. J. 1972, in *Gravitational N-Body Problem*, ed. M. Lecar (Dordrecht: Reidel), p. 373.
Aarseth, S. J., and Binney, J. 1978, *M.N.R.A.S.*, **185**, 227.
Aarseth, S. J., and Dekel, A. 1983, in preparation.
Ahmad, A., and Cohen, L. 1973, *J. Comp. Phys.*, **12**, 389.
Bahcall, N. 1981, *Ap. J.*, **247**, 787.
Binney, N. 1977, *Ap. J.*, **215**, 492.
Binney, J., and Silk, J. 1979, *M.N.R.A.S.*, **188**, 273.
Blumenthal, G. R., Pagels, H., and Primack, J. R. 1982, preprint.
Bond, J. R., Efstathiou, G., and Silk, J. 1980, *Phys. Rev. Letters*, **45**, 1980.
Bond, J. R., and Szalay, A. S. 1981, preprint.
Bond J. R., Szalay, A. S., and Turner, M. 1982, *Phys. Rev. Letters*, in press.
Chincarini, G., and Rood, H. J. 1979, *Ap. J.*, **230**, 648.
Davis, M., Frenk, C., and White, S. D. M. 1982, preprint.
Dekel, A. 1981, *Astr. Ap.*, **101**, 79.
_____. 1982, *Ap. J. (Letters)*, **261**, L13.
_____. 1983*a*, in preparation.
_____. 1983*b*, in preparation.
_____. 1983*c*, in preparation.
Dekel, A., and Aarseth, S. J. 1983, in preparation.
de Vaucouleurs, G. 1978, in *IAU Symposium 79, The Large Scale Structure of the Universe*, ed. M. S. Longair and J. Einasto (Dordrecht: Reidel), p. 205.
Doroshkevich, A. G. 1970, *Astrofizika*, **6**, 581.
Doroshkevich, A. G., Kotok, E. V., Novikov, I. D., Polyudov, A. N., Shandarin, S. F., and Sigov, Yu. S. 1980, *M.N.R.A.S.*, **192**, 321.
Doroshkevich, A. G., Khlopov, M. Yu, Sunyaev, R. A., Szalay, A. S., and Zel'dovich, Ya. B. 1981, in the *Proc. 10th Texas Symposium on Relativistic Astrophysics*, ed. R. Ramaty and F. C. Jones (*Ann. NY Acad Sci.*, **375**, 32).
Doroshkevich, A. G., Shandarin, S. F., and Saar, E. 1978, *M.N.R.A.S.*, **184**, 643.
Einasto, J., Joeveer, M., and Saar, E. 1980, *Nature*, **283**, 47.
Ford, H. C., Harms, R. J., Ciardullo, R., and Bartko, F., 1981, *Ap. J. (Letters)*, **245**, L53.
Gregory, S. A., Thompson, L. A., and Tifft, W. G., 1981, *Ap. J.*, **243**, 411.
Icke, V. 1973, *Astr. Ap.*, **27**, 1.
Kaastra, J. S., and van Bueren, H. G. 1981, *Astr. Ap.*, **99**, 7.
Kirshner, R. P., Oemler, A., Schechter, P. L., and Shectman, S. A. 1981, *Ap. J. (Letters)*, **248**, L57.
Klypin, A. A. 1980, *Astr. Zh.*, **57**, 913.
Klypin, A. A., and Shandarin, S. F. 1982, preprint.
Lin, C. C., Mestel, L., and Shu, F. H. 1965, *Ap. J.*, **142**, 1431.
Lynden-Bell, D. 1962, *Proc. Cambridge Phil. Soc.*, **58**, 709.
Melott, A. L. 1983*a*, *Ap. J.*, **264**, in press.
_____. 1983*b*, preprint.
Oort, J. H. 1970, *Astr. Ap.*, **7**, 381.
_____. 1982, preprint (*Ann. Rev. Astr. Ap.*, Vol. **21**).
Peebles, P. J. E. 1974, *Ap. J. (Letters)*, **189**, L51.
_____. 1981*a*, *Ap. J. (Letters)*, **243**, L119.
_____. 1981*b*, *Ap. J.*, **248**, 885.
Peebles, P. J. E., and Dicke, R. H. 1968, *Ap. J.*, **154**, 892.
Peebles, P. J. E., and Yu, J. T. 1970, *Ap. J.*, **162**, 815.
Press, W. H., and Davis, M. 1982, *Ap. J.*, **259**, 449.
Press, W. H., and Vishnaic, E. T. 1980, *Ap. J.*, **236**, 323.
Rees, M. J., and Kashlinski, A. 1982, preprint.
Rivolo, A., and Yahil, A. 1982, *Ap. J.*, **251**, 457.
Sandage, A., and Tammann, G. A. 1981, *Revised Shapley-Ames Catalog* (Washington: Carnegie Institution of Washington).
Silk, J. 1968, *Ap. J.*, **151**, 459.
Silk, J., and Wilson, M. L. 1980, *Phys. Scripta*, **21**, 708.
_____. 1981, *Ap. J. (Letters)*, **244**, L37.
Sunyaev, R. A., and Zel'dovich, Ya B. 1972, *Astr. Ap.*, **20**, 189.
Tarenghi, M., Tifft, W. G., Chincarini, G., Rood, H. J., and Thompson, L. A., 1979, *Ap. J.*, **234**, 793.
Tully, R. B. 1982, *Ap. J.*, **257**, 389.
Tully, R. B., and Fisher, J. R. 1982, Atlas and Catalog of Nearby Galaxies, in preparation.
White, S. D. M. 1978, *M.N.R.A.S.*, **184**, 185.
White, S. D. M., and Rees, M. J., 1978, *M.N.R.A.S.*, **183**, 341.
White, S. D. M., and Silk, J. 1979, *Ap. J.*, **231**, 1.
Yahil, A., Sandage, A., and Tammann, G. A., 1980, *Ap. J.*, **242**, 448 (YST).
Zel'dovich, Ya B. 1970, *Astr. Ap.*, **5**, 84.
_____. 1978, in *IAU Symposium No. 79, The Large Scale Structure of the Universe*, ed. M. S. Longair and J. Einasto (Dordrecht: Reidel), p. 409.

AVISHAI DEKEL: Astronomy Department, Yale University, Box 6666, New Haven, CT 06511